Spatial Uniformity Study in a Loaded Reverberation Chamber at Millimeter-Wave Frequencies

Damir Senic, Kate A. Remley, Maria G. Becker, and Christopher L. Holloway
National Institute of Standards and Technology
Boulder, CO
damir.senic@nist.gov

***Abstract*—We performed a study of the spatial uniformity of the averaged fields in a reverberation chamber at millimeter-wave frequencies based on measurements of the power transfer function for six different reverberation chamber loading configurations. We show that chamber spatial uniformity is strongly influenced by loading. An unloaded chamber can be considered as a nearly uniform environment, while uniformity decreases with increased loading. The loading of a chamber is key for wireless tests involving modulated signals. Its purpose is to create a frequency-flat channel, which enables successful demodulation of the signal without distortion. Consequently, understanding this effect is important in quantifying measurement uncertainty in loaded conditions.**

Keywords—measurements uncertainty; reverberation chamber; RF loading; spatial uniformity; wireless systems

I. INTRODUCTION

Reverberation chambers (RCs) have been traditionally used for various electromagnetic compatibility (EMC) measurements since the 1980s. Recently, they have become important to the wireless industry for over-the-air (OTA) tests of wireless devices such as smartphones, machine-to-machine (M2M) and internet-of-things (IoT) devices.

Reverberation chambers are electrically-large resonators where, when averaged over a mode-stirring sequence, fields ideally have a spatially-uniform distribution [1]. Spatial uniformity in RCs has been studied previously [2]-[11]. However, those studies did not investigate the decrease in uniformity that occurs when a chamber is loaded in order to flatten its frequency response.

Empirical study of real reverberation chamber spatial uniformity is particularly interesting to the wireless community, which employs RCs for OTA tests [3], [12]. The key difference between traditional EMC tests deploying continuous-wave signals and wireless tests of modulated signals is that wireless tests generally require a loaded chamber to mimic a realistic channel coherence bandwidth (CBW). RF loading creates a channel with fading characteristics [13] that act like a real channel for which the device is designed to operate in. Loading broadens and flattens the frequency response of the channel inside the chamber by increasing the CBW, which is necessary for demodulating modulated signals without distortion [4],[14]. However, heavy loading, if not properly accounted for in stirring sequence design, may have negative impacts on the chamber's behavior, as it decreases spatial uniformity and increases chamber anisotropy [15] due primarily to the unstirred multipath components. Common practice for wireless measurements involving RCs is to minimize unstirred energy by applying additional spatial stirring mechanisms (antenna platform stirring and antenna polarization stirring) in addition to paddle stirring, and by optimizing the antenna placement and orientation inside the chamber [4].

A real RC setup will exhibit some lack of spatial uniformity depending on the amount of loading. Field uniformity is an important figure of merit in standardized tests [12],[16]. A common way to characterize the chamber uniformity is to measure the electric field or received power at different locations using a field probe or an antenna. One method for performing field uniformity characterization of a reverberation chamber is described in the IEC 61000-4-21 standard [16]. The IEC test specifies electric-field measurements with an electric-field probe or power measurements with an antenna at eight different locations inside the chamber that form the edge of the chamber's working volume. Electric-field probes are suggested because they have small dimensions and, therefore, should not significantly perturb the fields inside the chamber. The small size of the field probe also means that undesirable field averaging typical of larger antennas, can be avoided. In [12], the chamber power transfer function is measured with a reference antenna that has "similar" radiation characteristics as the device under test (DUT). Measurements are conducted at nine spatially-independent locations, where independence is confirmed through cross correlation.

In the present work, we extend the work of [4],[17] by use of the method of [12] to study a chamber operating at millimeter-wave frequencies. The reverberation chamber environment is evaluated by measuring the chamber's power transfer function for different loading cases at nine locations inside the chamber (see Fig. 1). We compare the results to lower-frequency measurements performed inside a chamber operating at microwave frequencies. The results indicate that the extremely high-Q of the millimeter-wave chamber provides a lower standard deviation in the chamber power transfer function between nine antenna locations for a given coherence bandwidth due to its rich modal characteristics. Consequently, since CBW increases with frequency, a millimeter-wave chamber is capable of achieving a broader CBW than a reverberation chamber operating at microwave frequencies, which should be very useful for future generation (5G) wireless OTA tests involving reverberation chambers.

* Work supported by U.S. government, not protected by U.S. copyright

II. Measurement Configuration and Chamber Characterization

We performed spatial uniformity measurements with a 50 GHz VNA in terms of the chamber power transfer function (G_{ref}) for the tabletop-sized reverberation chamber shown in Figs. 1 and 2. The chamber's power transfer function (G_{ref}) is defined as

$$G_{\text{ref}} = \frac{\left\langle |S_{21}|^2 \right\rangle}{\eta_{\text{TX}}\eta_{\text{RX}}\left(1-\left|\langle S_{11}\rangle\right|^2\right)\left(1-\left|\langle S_{22}\rangle\right|^2\right)}, \qquad (1)$$

where the brackets denote the ensemble average over the mode-stirring sequence, S_{21} is the forward transmission scattering parameter measured by a VNA, and the terms in the denominator represent the free-space radiation efficiencies (η_{TX} and η_{RX}) and mismatch corrections for the two antennas. The radiation efficiency can be measured in either an anechoic chamber or in an unloaded reverberation chamber [5].

Our chamber is equipped with two mechanical stirrers. The larger one rotates about a horizontal (H) axis within a cylindrical volume of 0.6 m height and 0.2 m diameter, while the smaller one rotates about a vertical (V) axis within a cylindrical volume of 0.5 m height and 0.2 m diameter. The RC's inner dimensions are 1 m (l) × 0.65 m (w) × 0.55 m (h), which corresponds to an electrical size of approximately 150 λ × 100 λ × 80 λ, at 45 GHz. This is important to emphasize since the high operating frequency results in a large electrical size for the RC, despite its small physical size. All measurements are made in the stepped mode under steady state conditions.

The RC's bulkhead was equipped with two feedthroughs, one in waveguide that was connected through a coax-to-waveguide adapter to the VNA's port 2 and the other in a 2.4 mm coax that was connected to the VNA's port 1. The port 2 bulkhead was terminated with the receive WR22 Q-band waveguide horn antenna oriented toward the vertical stirrer (see Figs. 1 and 2). The signal from the 2.4 mm coaxial feedthrough was brought to an identical transmit waveguide horn antenna via a coaxial cable and coax-to-waveguide transition. The receive and transmit antennas were oriented away from each other in order to minimize the direct signal component between them. The transmit antenna was oriented toward the horizontal stirrer and positioned at nine different locations within the RC's working volume (see Figs. 1 and 2) in order to measure the distribution of received power inside the RC for different loading configurations. Key measurement parameters are summarized in Table I. A schematic representation of the measurement setup is given in Fig. 1.

To study the effect of chamber loading on spatial uniformity, measurements were repeated for six different loading configurations: an empty RC and the RC loaded with one, three, six, ten and fourteen pyramidally shaped RF absorber blocks, as shown in Fig. 2. The absorbers had dimensions of 15 cm (l) × 15 cm (w) × 7.5 cm (h). Absorber layout and orientation are shown in Figs. 1 and 2.

Chamber loading decreases the chamber Q factor by increasing the loss inside the chamber and broadens the chamber's CBW by increasing correlations between frequencies [4],[18]. Loading also increases the correlations between stirrer positions which reduces the maximum number of independent paddle samples.

The CBW represents the average bandwidth over which signals measured at neighboring frequencies exhibit correlation above a specified threshold. The CBW can be determined from the autocorrelation function (R) of the frequency-domain transfer function S_{21} [16],[18] given by

$$R\left(\Delta f_i, n_i\right) = \sum_{j=1}^{m} S_{21}\left(f_j, n_i\right) S_{21}^{*}\left(f_j + \Delta f_i, n_i\right), \qquad (2)$$

where $S_{21}(f, n)$ corresponds to the measured complex S_{21} at frequency step f_j with m frequency points measured within the bandwidth of interest, Δf corresponds to one of several frequency offsets over the bandwidth of interest, the index n_i is the mode-stirring sample (out of N), and the asterisk denotes complex conjugation.

The CBWs at 45 GHz (calculated for 1 GHz bandwidth) for the six loading configurations calculated for three different typical thresholds (1/e, 0.5, and 0.7) are shown in Fig. 3 and summarized in Table II. Different standards use different thresholds. Therefore, we present the results of our CBW study for three different thresholds.

TABLE I. Measurement Parameters

Parameter	Value
Frequency range	43 GHz – 47 GHz
Number of frequency points	1601
VNA IF bandwidth	2 kHz
VNA output power level	-10 dBm
VNA dwell time	100 μs
VNA sweep delay time	10 μs
Paddle step size ($V \times H$)	7.2° × 7.2°
Number of paddle positions-stepped ($V \times H$)	50 × 50 = 2,500

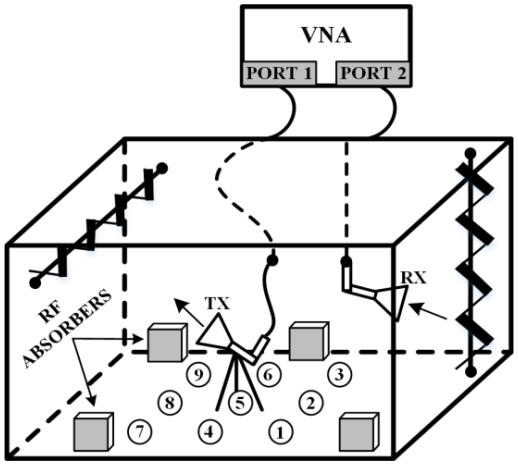

Fig. 1. Schematic of chamber setup for spatial uniformity measurements. Locations 1, 2, …, 9 reperesent the testing locations of the trasnmit antenna TX.

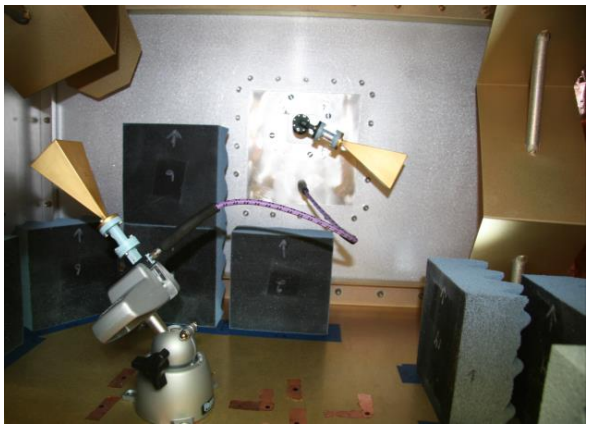

Fig. 2. Heavily loaded chamber setup showing RF absorber blocks and placement and orientation of transmit and receive antennas.

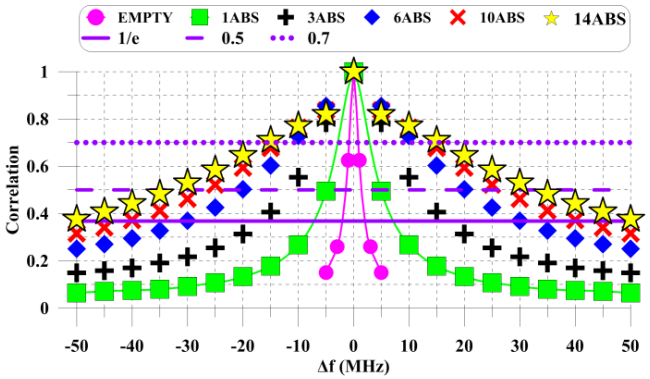

Fig. 3. Coherence bandwidth results at 45 GHz for the six loading configurations calculated for three different thresholds.

TABLE II. COHERENCE BANDWIDTH RESULTS FOR SIX LOADING CONFIGURATIONS AT 45 GHZ

Loading	CBW (MHz)		
	1/*e*	0.5	0.7
Empty	4	3	2
1 Absorber	15	10	5
3 Absorbers	35	24	14
6 Absorbers	60	40	22
10 Absorber	80	54	26
14 Absorbers	100	65	30

III. MEASUREMENTS OF SPATIAL UNIFORMITY

To study the RC's spatial uniformity as a function of loading, we used the method of [12],[16]. The chamber transfer function (G_{ref}) from (1) was calculated for six different chamber loading configurations and at nine transmit antenna locations. Placement of the RF absorbers inside the chamber can be seen in Fig. 2. The horn antenna efficiencies were previously measured with the method of [5]. The G_{ref} results, averaged over the 4 GHz band (43 GHz – 47 GHz), are shown in Fig. 4 at each TX antenna location and for each chamber loading configuration.

G_{ref} values averaged over nine antenna locations together with Rician K factor values are given in Table III. The K factor metric describes the unstirred energy present inside the RC which is defined as the ratio of unstirred to stirred power and can be estimated from S-parameters as

$$K = \frac{\left|\langle S_{21}\rangle\right|^2}{\left\langle\left|S_{21}-\langle S_{21}\rangle^2\right|\right\rangle}. \quad (3)$$

Generally, the unstirred energy is defined as the part of the total energy available inside the RC that reaches the receive antenna without prior interaction with paddles. The existence of the unstirred energy leads to the creation of "hot spots" which reduce spatial uniformity. In this case, additional stirring mechanisms, such as antenna platform stirring, need to be applied. The presence of RF absorbing material inside the RC reduces the total available stirred energy which is exhibited as poor stirring efficiency and a higher K factor, as shown in Table III.

TABLE III. G_{REF} AND K-FACTOR RESULTS AT 45 GHZ FOR SIX LOADING CONFIGURATIONS AVERGAED OVER NINE ANTENNA LOCATIONS AND A 4 GHZ BAND

Loading	G_{ref} (dB)	K (dB)
Empty	-35.54	-28.25
1 Absorber	-41.60	-21.96
3 Absorbers	-45.30	-19.58
6 Absorbers	-48.28	-18.84
10 Absorber	-49.93	-18.80
14 Absorbers	-51.03	-18.25

Next, we studied the standard deviation in G_{ref} between the nine antenna locations for different RC loading configurations given in Fig. 5 which illustrates the trend of decreased uniformity with increased loading. More loading creates stronger "hot spots" in the observed volume, thus causing larger deviations in the measured quantity with respect to the antenna location.

The unloaded chamber provides a nearly-uniform field distribution throughout the observed volume with a standard deviation of 0.02 dB between G_{ref} measured at nine different locations. By adding loading inside the RC, the standard deviation in G_{ref} increased from 0.06 dB, calculated for one RF absorber present inside the RC, to 0.27 dB for 14 RF absorbers. Based on the uncertainty analyses given in the next section, this illustrates the need to apply antenna location stirring for wireless tests in order to keep the uncertainty below 0.2 dB (~5%).

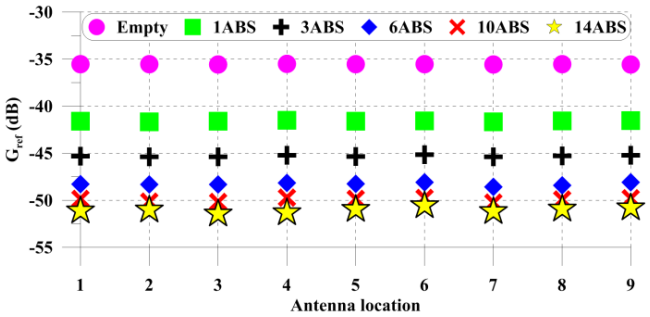

Fig. 4. G_{ref} measured over 4 GHz band (43 GHz – 47 GHz) and averaged over nine TX antenna locations for six different loading configurations.

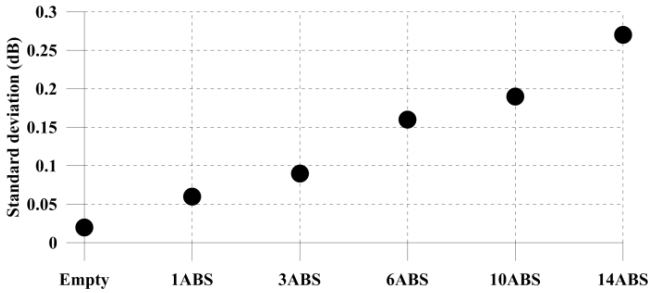

Fig. 5. Standard deviation in G_{ref} between nine antenna locations for six different loading configurations.

Next, we compare these results to a chamber operating at microwave frequencies [15]. G_{ref} measurements were performed at ten different locations inside a 1.9 m (l) × 1.4 m (w) × 2 m (h) reverberation chamber over the Personal Communications Service (PCS) band (1850 MHz – 1990 MHz) with a half-wavelength dipole receive antenna. As a transmit antenna, we used a broadband (650 MHz – 3.5 GHz) discone monopole. In order to study the effect of chamber loading on spatial uniformity, measurements were repeated for three different chamber loading configurations: unloaded, partially loaded, and heavily loaded. For the heavily-loaded case, we used five large absorbers with dimensions of 15 cm (l) × 6 cm (w) × 60 cm (h), and four small absorbers with dimensions of 15 cm (l) × 6 cm (w) × 15 cm (h). The partially-loaded chamber had three large absorbers.

A comparison of these chambers is presented in Table IV in terms of the chamber power transfer function (G_{ref}), standard deviation of G_{ref} between different antenna locations, and CBW (1/e threshold). For all loading configurations, we see a higher standard deviation in G_{ref} for the reverberation chamber operating at microwave frequencies compared to the millimeter-wave chamber. The reason for this is the extremely high mode density of the millimeter-wave chamber where, even though the chamber is heavily loaded, it still preserves its rich modal characteristic where modes overlap at a much higher rate causing more modes to participate in reinforcing the randomness of the EM field, which results in better spatial uniformity. On the other hand, spatial uniformity of the undermoded chamber operating at microwave frequencies is greatly compromised by adding RF absorbers.

Table IV also shows that the CBW values are much lower for the chamber operating at microwave frequencies due to larger distance between adjacent modes. This indicates that more RF loading is required in order to achieve sufficient CBW at microwave frequencies. For example, both empty chambers exhibit similar CBWs: 2.86 MHz for the microwave chamber and 4 MHz for the millimeter-wave chamber. However, once when we start adding RF absorber to the chamber, the differences become significant: the heavily-loaded microwave chamber configuration has a CBW of 12.26 MHz, which is exceeded with only one absorber in the case of the millimeter-wave RC. Hence, the millimeter-wave chamber provides much broader CBWs (up to 100 MHz with a 1/e threshold in our study) as compared to the traditional microwave RC. This indicates that the millimeter-wave chamber is a good candidate for the OTA tests of future 5G modulated signals whose bandwidth will be much broader than today's signals, which are only a few megahertz.

Note that these two chambers have very different Q factors when not loaded. Therefore, more comprehensive study would involve a comparison based on the absorbers' absorption cross sections. Here, our main point is to show a potential RC application for millimeter-wave wireless communications tests.

TABLE IV. G_{REF}, STANDARD DEVIATION IN G_{REF}, AND COHERENCE BANDWIDTH FOR REVERBERATION CHAMBERS OPERATING AT MICROWAVE AND MILLIMETER-WAVE FREQUENCIES

Frequency range	Loading	G_{ref} (dB)	σ (dB)	CBW (MHz)
Microwave	Empty	-17.60	0.25	2.86
	Partially loaded	-21.12	0.39	7.76
	Heavily loaded	-24.53	0.97	12.26
Millimeter-wave	Empty	-35.54	0.02	4
	1 Absorber	-41.60	0.06	15
	3 Absorbers	-45.30	0.09	35

IV. UNCERTAINTY IN THE ESTIMATE OF G_{REF}

In tests involving loaded reverberation chambers, we generally distinguish between two key sources of uncertainty: (1) the uncertainty due to the finite number of mode-stirred measurement samples, within a given mode-stirring sequence, and (2) the uncertainty due to the lack of spatial uniformity of the averaged fields in the chamber, which originates between different antenna locations in the chamber.

In wireless tests, where chambers are often loaded, it is common that the uncertainty due to lack of spatial uniformity dominates, compared to the uncertainty arising from the finite number of mode-stirred samples in a mode-stirring sequence [17]. However, for low-loss (high-Q) unloaded RCs, this is not always the case [6], and the relative effects of these two contributions should be studied. Therefore, we need to find the uncertainties associated with the number of mode-stirred samples N (2,500 in our setup) and the uniformity for M (nine in our setup) measurement antenna locations.

In the previous section, we showed by calculating the standard deviation in G_{ref} that loading deteriorates spatial uniformity. Hence, we expect that the uncertainty due to lack of spatial uniformity will dominate the overall uncertainty for a highly loaded chamber. To determine which RC-induced component of the uncertainty is dominant, a significance test may be performed [17].

The outcome of the significance test provides us with a metric for determining the correct expression for standard uncertainty in G_{ref} measurements for a given chamber setup. The statistics for testing the significance of each uncertainty are based on an F distribution and given by [19]

$$\mathrm{F}\left(s_M^2, s_N^2\right) = \frac{s_M^2}{s_N^2}, \tag{4}$$

with M – 1 and M (N – 1) degrees of freedom. The mean-squared deviation due to the mode-stirred samples is denoted by s_N^2, and the mean-squared deviation due to the lack of

spatial uniformity is denoted by s_M^2. The expressions for calculating s_N^2 and s_M^2 can be found in [17].

The significance test can have two possible outcomes: (1) the uncertainty due to lack of spatial uniformity is not significant; *i.e.*,

$$\mathrm{F}\left(s_M^2, s_N^2\right) < \mathrm{F}_{\alpha, n_1, n_2}, \tag{5}$$

where α is the confidence level (*e.g.*, 95%), and $n_1 = M - 1$ and $n_2 = M\,(N - 1)$ are degrees of freedom, or
(2) the uncertainty due to lack of spatial uniformity is significant; *i.e.*,

$$\mathrm{F}\left(s_M^2, s_N^2\right) > \mathrm{F}_{\alpha, n_1, n_2}. \tag{6}$$

In the first case, the uncertainty of the reference value is given as

$$u_{\mathrm{ref}} = \sqrt{\frac{\sum_{i=1}^{N}\sum_{j=1}^{M}\left[G_{\mathrm{ref}}\left(n_i, m_j\right) - \left\langle G_{\mathrm{ref}}\right\rangle_{N,M}\right]^2}{NM\left(NM-1\right)}}, \tag{7}$$

while in the second case, the uncertainty should be determined from

$$u_{\mathrm{ref}} = \sqrt{\frac{\sum_{j=1}^{M}\left[\left\langle G_{\mathrm{ref}}\left(m_j\right)\right\rangle_N - \left\langle G_{\mathrm{ref}}\right\rangle_{N,M}\right]^2}{M\left(M-1\right)}}. \tag{8}$$

The uncertainty results based on the significance test are presented in Table V, where the decibel representation of normalized uncertainty was calculated as

$$u_{\mathrm{ref}}^{\mathrm{dB}} = 10\log_{10}\left(\frac{G_{\mathrm{ref}} + u_{\mathrm{ref}}}{G_{\mathrm{ref}}}\right). \tag{9}$$

TABLE V. SIGNIFICANCE TEST RESULTS AND COMPARISON WITH F DISTRIBUTION CONFIDENCE LEVEL OF 95%

Loading	$\mathbf{F_{0.95,\,8,\,22491} = 1.94}$	u_{ref} **(dB)**	u_{ref} **(%)**
Empty	0.001 NOT SIGNIFICANT	0.05	1.16
1 Absorber	0.06 NOT SIGNIFICANT	0.06	1.29
3 Absorbers	1.49 NOT SIGNIFICANT	0.13	2.93
6 Absorbers	2.09 SIGNIFICANT	0.19	4.45
10 Absorber	2.88 SIGNIFICANT	0.25	5.89
14 Absorbers	3.57 SIGNIFICANT	0.31	7.35

The significance test showed that the uncertainty due to lack of spatial uniformity is not significant for the empty millimeter-wave chamber or the chamber loaded with one or three RF absorbers. For these cases, we calculated the uncertainty in our estimate of G_{ref} from (7) as 1.16% for the empty RC, 1.29% for the RC loaded with one absorber, and 2.93% for the RC loaded with three absorbers. By adding more loading inside the RC, the uncertainty due to lack of spatial uniformity becomes dominant and we need to use (8) in order to calculate the uncertainty of the reference value. Calculated uncertainties were 4.45%, 5.89%, and 7.35% for six absorbers, ten absorbers, and fourteen absorbers, respectively. For the proposed F test, we used a 95% confidence level with $n_1 = 8$, and $n_2 = 2{,}2491$ degrees of freedom, which resulted in a value of 1.94. Other confidence levels with different F test values can be used as well. Please note that we did not study the impact of the absorber's geometry and position inside the RC on the G_{ref} uncertainty.

Please note that we report here only the uncertainty due to the finite number of mode-stirred measurement samples, within a given mode-stirring sequence, and the uncertainty due to the lack of spatial uniformity of the averaged fields in the chamber, which originates between different antenna locations in the chamber. The other sources of the uncertainty, such as cable movement, were not studied in this paper. The readers interested in more comprehensive uncertainty budget for similar test setup are referred to [5].

V. CONCLUSION

In this paper, we presented an RC spatial uniformity study for six different loading configurations: an empty chamber and a chamber loaded with one, three, six, ten, and fourteen absorbers. In an ideal chamber, the fields are uniformly distributed throughout the observed volume when averaged over a stirring sequence. The empty chamber studied here provided a nearly-uniform field distribution similar to the ideal chamber. By adding RF loading inside the RC, the spatial uniformity deteriorated in such a way that the standard deviation in G_{ref} measurements increased from 0.06 dB for one absorber to 0.27 dB in the case of the chamber loaded with the maximum of fourteen absorbers. The former caused an increase of uncertainty in the estimate of G_{ref} from 1.16% to 7.31%. Hence, in order to create practical measurements involving heavier loading configurations, we generally need to apply antenna location stirring, otherwise measurements will be strongly location dependent.

Next, we made a comparison of spatial uniformity measurements between reverberation chambers operating at microwave and millimeter-wave frequencies. The results showed a significantly higher standard deviation in G_{ref} measured at different antenna locations for all loading configurations. Also, the chamber operating at millimeter-wave frequencies had a much broader CBW compared to that of the microwave chamber.

RF absorbers load the chamber and lower the number of excited modes. In the case of heavily-loaded chambers, modes can have different distributions which can be analytically studied. In this paper, we did not perform such a study which has much interest for the future. In future work, we will use the findings from chamber characterization presented here, in particular the CBW and uncertainty analyses, to perform true OTA measurements of modulated signals at millimeter-wave frequencies.

REFERENCES

[1] D. A. Hill, *Electromagnetic Fields in Cavities*, Piscataway: Wiley IEEE Press, 2009.

[2] C. L. Holloway, D. A. Hill, J. M. Ladbury, and T. M. Lammers, "Assessing loaded reverberation chambers: calculating threshold metrics," *IEEE International Symposium on Electromagnetic Compatibility* 2003, pp. 834–837.

[3] P.-S. Kildal, X. Chen, C. Orlenius, M. Franzen, and C. S. L. Patane, "Characterization of reverberation chambers for OTA measurements of wireles devices: Physical formulation of channel matrix and new uncertainty formula," *IEEE Trans. Antennas and Propag.*, vol. 60, no. 8, pp. 3875–3891, Aug. 2012.

[4] K. A. Remley, J. Dortmans, C. Weldon, R. D. Horansky, T. B. Meurs, C.-M. Wang, D. F. Williams, C. L. Holloway, and P. F. Wilson, "Configuring and verifying reverberation chambers for testing cellular wirelss devices," *IEEE Trans. Electromagn. Compat.*, vol. 58, no. 3, pp. 661–672, June 2016.

[5] D. Senic, D. F. Williams, K. A. Remley, C.-M. Wang, C. L. Holloway, Z. Yang, and K. F. Warnick, "Improved antenna efficiency measurement uncertainty in a reverberation chamber at millimeter-wave frequencies," *IEEE Trans. Antennas Propag*., vol. 65, no. 8, pp. 4209–4219, Aug. 2017.

[6] D. Senic, K. A. Remley, C.-M. Wang, D. F. Williams, C. L. Holloway, D. C. Ribeiro, and A. T. Kirk, "Estimating and reducing uncertainty in reverberation-chamber characterization at millimeter-wave frequencies," *IEEE Trans. Antennas and Propag.*, vol. 64, no. 7, pp. 3130–3140, Jul. 2016.

[7] K. Harima and Y. Yamanaka, "Evaluation of e-field uniformity for radiated immunity testing in a reverberation chamber," *IEEE International Symposium on Electromagnetic Compatibility* 2001, pp. 768–770.

[8] Y. J. Wang, W. J. Koh, Y. K. Tai, C. K. Lee, and K. Y. See, "Evaluating field uniformity of a mini-reverberation chamber with two mechanical stirrers," *IEEE International Symposium on Electromagnetic Compatibility* 2002, pp. 795–798.

[9] B. Zhang, W. Li, X. Li, Z. Yuan, J. He, and R. Zeng, "Field uniformity investigation of reverberation chamber at calibration stage," *IEEE International Symposium on Electromagnetic Compatibility (EMC Europe)* 2009, pp. 45–48.

[10] V. M. Primiani and F. Moglie, "Numerical determination of reverberation chamber field uniformity by a 3-D simulation," *IEEE International Symposium on Electromagnetic Compatibility (EMC Europe)* 2011, pp. 829–832.

[11] T. Hui, F. Chonghua, H. Mingliang, and T. Li, "Numerical simulation of field uniformity of reverberation chamber," *International Symposium on Antennas, Propagation and EM Theory (ISAPE)* 2016, pp. 481–484.

[12] CTIA Certification, "Test Plan for Wireless Large-Form-Factor Device Over-the-Air Performance" Oct. 2016.

[13] A. Goldsmith, *Wireless Communications*. Cambridge, U.K.: Cambridge Univ. Press, 2005.

[14] J. N. H. Dortmans, K. A. Remley, D. Senic, C.-M. Wang, C. L. Holloway, "Use of absorption cross section to predict coherence bandwidth and other characteristics of a reverberation chamber setup for wireless-system tests," *IEEE Trans. Electromagn. Compat.*, vol. 58, no. 5, pp. 1653–1661, Oct. 2016.

[15] D. Senic, D. Cavaliere, M. V. North, M. G. Becker, K. A. Remley, C.-M. Wang, and C. L. Holloway, "Isotropy study for Over-the-Air measurements in a loaded reverberation chamber," *IEEE International Symposium on Electromagnetic Compatibility and Signal/Power Integrity (EMCSI)* 2017, pp. 124–129.

[16] "IEC 61000-4-21: EMC, Part 4: Testing and Measurement Techniques; Section 21: Reverberation Chamber Test Methods," *Int. Electrotech. Comm*., Geneva, 2011.

[17] K. A. Remley, C.-M. Wang, D. F. Williams, J. Aan Den Toorn, and C. L. Holloway, "A significance test for reverberation-chamber measurement uncertainty in total radiated power of wireless devices", *IEEE Trans. Electromagn. Compat.*, vol. 58, no. 1, pp. 207–219, February 2016.

[18] X. Chen, P.-S. Kildal, C. Orlenius, and J. Carlsson, "Channel sounding of loaded reverberation chamber for over-the-air testing of wireless devices: Coherence bandwidth versus average mode bandwidth and delay spread," *IEEE Antennas Wireless Propag. Lett.*, vol. 8, pp. 678-681, Jun. 2009.

[19] Joint Committee for Guides in Metrology, "Evaluation of measurement data—Guide to the expression of uncertainty in measurement," International Bureau of Weights and Measures (BIPM): Sèvres, France, September 2008.